Servo Motor Size Reduction - Need for Thermal CAD

Dr.D.A.Staton
Director
Motor Design Ltd
UK
Tel: +44 1691 623305
dave.staton@motor-design.com
www.motor-design.com

INTRODUCTION

There is currently a revolution in the development of compact brushless permanent magnet (BPM) servo motors which are up to 75% of the size of conventional products [1-6]. Such large size reductions are due to a combination of factors including, modern manufacturing techniques, improved magnet grades, new materials and improved design capabilities. This paper will concentrate on the improvements that can be achieved by using advanced design capabilities. In particular it will concentrate on the thermal design of motors, a discipline that has traditionally received much less attention than electromagnetic design.

Traditionally the thermal performance of a new motor design has been estimated from prior knowledge of one or more of the following parameters - winding to ambient thermal resistance, housing heat transfer coefficient, winding current density limit or winding specific electric loading limit. These numbers may be estimated from tests on existing motors, from competitor catalogue data, or from simple rules of thumb [7-9]. The problem with such design methods is that no insight is gained of where the thermal design may be compromised and therefore where design effort should be concentrated.

One of the thermal modules of a new commercially available motor design package (Motor-CAD) will be the focus of this paper. This module (BPM-Therm), can be used to give the designer a rapid method of analysing design changes on the thermal behaviour of BPM motors. In doing so, not only can the optimum design solution be quickly identified, but the user fully understands the consequences of changes. It will be used to examine a selection of the thermal issues that may be considered when designing a new motor. It will also be used to highlight some of the improvements that can be achieved by adopting some of the new manufacturing techniques and materials available. Data is presented to illustrate improvements achieved in particular designs. These values cannot however be generalised to all motors as each design is different and a complete thermal evaluation should be performed on all new designs.

The use of Motor-CAD in the design process reduces the requirement for prototypes. Prototype building gives an indication of the improvements that can be gained by altering the motor design, however, it does not give a direct indication of which components and design parameters have the most influence on the thermal design. This information is readily available using Motor-CAD.

MOTOR-CAD

The Motor-CAD thermal model is based upon lumped-circuit analysis. The lumped circuit approach has a clear advantage over numerical techniques such as finite-element analysis (FEA) and computational fluid dynamics (CFD) techniques in terms of calculation speed. The near instantaneous calculation capabilities of Motor-CAD make it possible to run "what-if" scenarios in real time. The main strengths of the numerical techniques are in the development of convection formulations for use in lump-circuit analysis [10,11], rather than carrying out the thermal circuit optimisation itself.

Lumped Circuit Schematic:

Fig 1 show typical schematic diagrams of a brushless permanent magnet motor model developed with Motor-CAD. A schematic diagram is useful for analysing steady-state thermal data. It is used to analyse thermal resistance, power flow and temperature distribution within the motor. Components are colour coded to match those shown in the cross-section editors (Fig's 2 to 5). In summary, the circuit consists of thermal resistances and heat sources connected between motor component nodes.

Thermal resistance values for all conduction paths within the motor are calculated from motor dimensions and material data. The accuracy of the calculation is dependent upon knowledge of the various thermal contact resistances between components within the motor, e.g. housing to lamination interface, slot-liner to lamination interface. Such resistances occur due to contact between solid surfaces taking place at limited numbers of high spots, the adjacent voids usually being filled with air. There has been much experimental work on the prediction of contact resistance [9, 12, 15]. The Motor-CAD online help system summarises this literature to include guidance on effective gaps to be expected with different material types, interface pressures and surface roughness. Motor-CAD combined with motor test data also forms an effective parameter identification tool. This technique can be used to estimate the gaps within the machine which are physically impossible to measure and to quantify the effects of winding impregnated air pockets.

When carrying out transient analysis, thermal capacitances are connected to each of the nodes within the schematic shown in Fig 1. Each capacitance is calculated from the specific heat capacity and weight of the relevant motor components. The resulting set of partial differential equations are integrated to obtain the thermal transient characteristics.
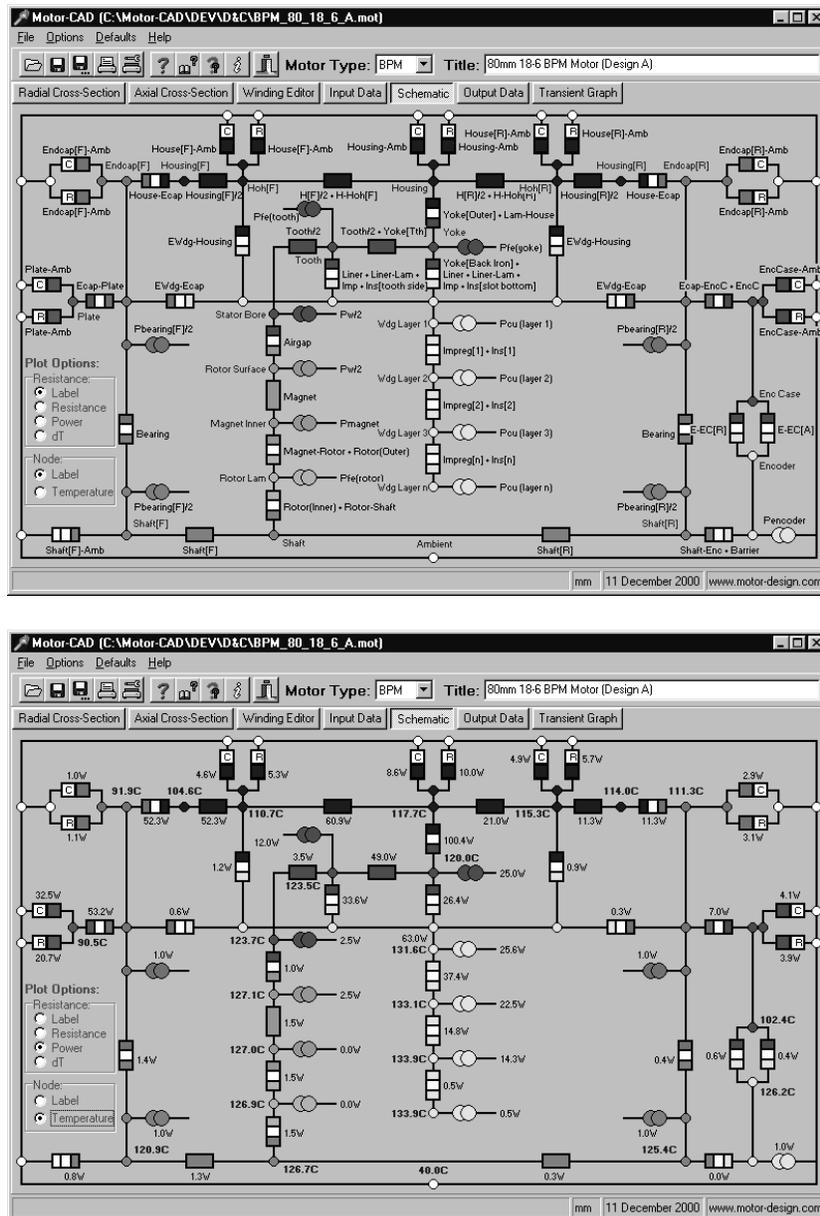

Fig. 1: Motor-CAD lumped circuit model showing resistance/node labels and power flow/nodal temperatures

Cross-Section Editor:

Radial & axial cross-section editors are used for dimensional data input (Figs 2 to 5). Figs 2 & 3 show two 80mm diameter designs, one based upon a traditional inserted winding, the second based upon a concentrated bobbin winding. The traditionally wound motor has 18 slots and 6 poles, while the concentrated winding motor has 12 slots and 8 poles. Both motors have the same diameter and active axial length, however, the traditionally wound motors overall length is 30% longer to accommodate the longer end-turns. Figs 4 & 5 show equivalent diagrams to Figs 2 & 3 but for 160mm diameter designs. In this case the traditionally wound motor has 36 slots & 6 poles and the concentrated winding motor has 12 slots & 8 poles. The overall length of the traditionally wound motor is 21% longer to accommodate the longer end-turns.
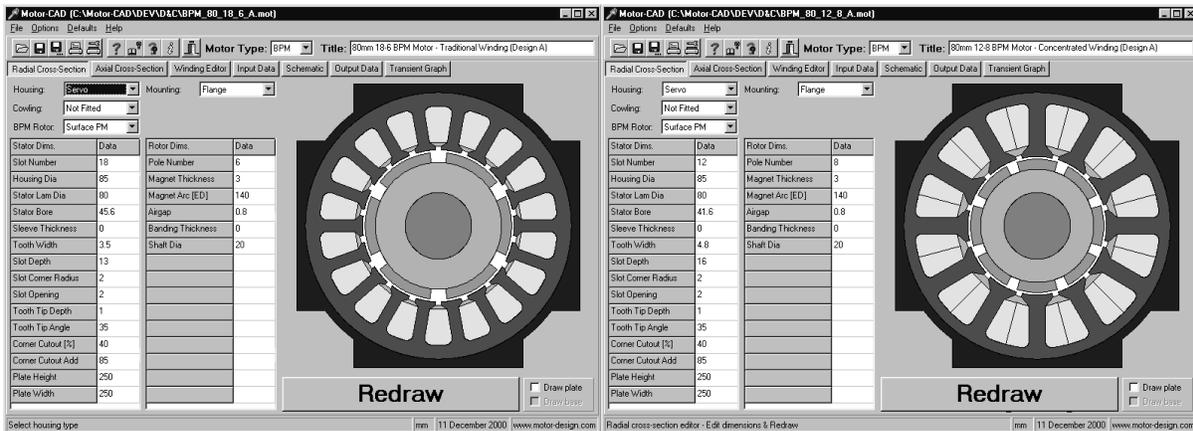

Fig. 2: Radial cross-section editor showing 80mm diameter traditional & concentrated winding motor designs
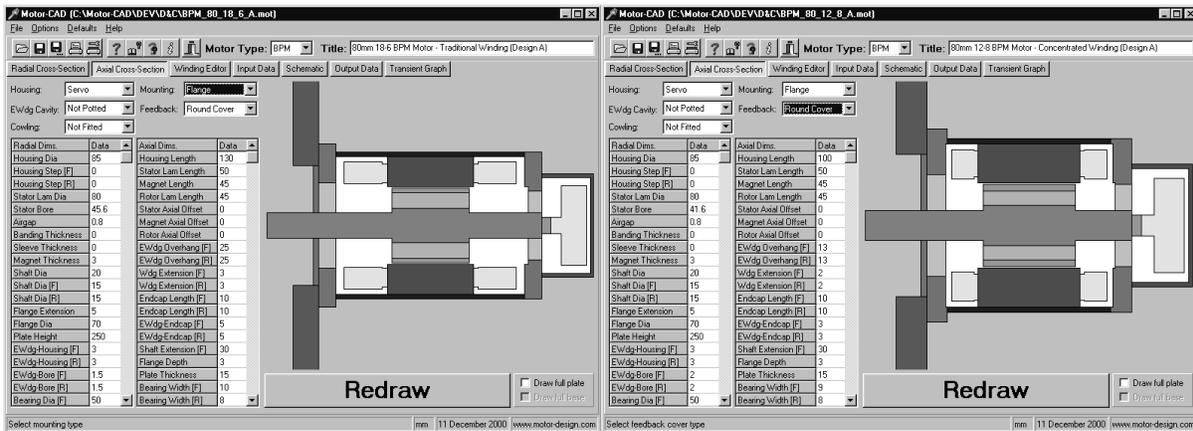

Fig. 3: Axial cross-section editor showing 80mm diameter traditional & concentrated winding motor designs
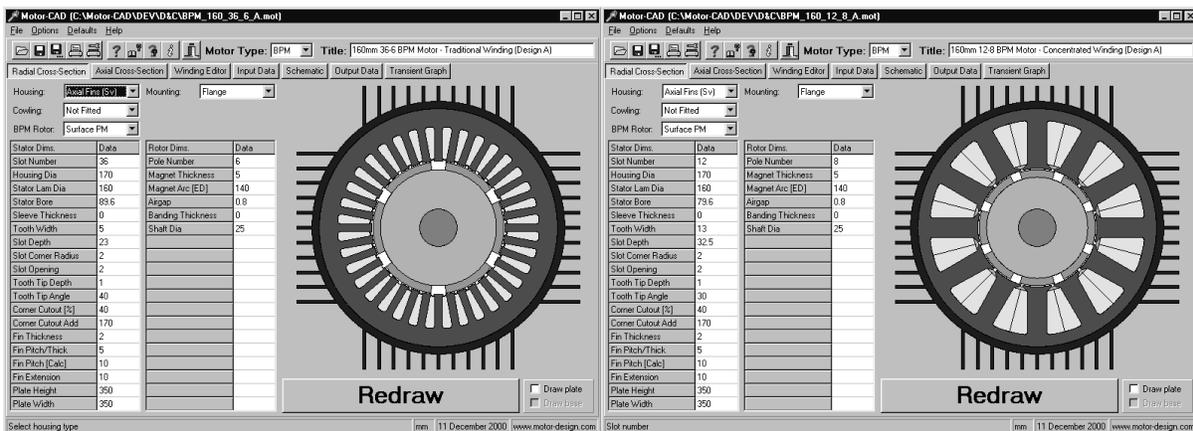

Fig. 4: Radial cross-section of 160mm diameter traditional & concentrated winding motor designs
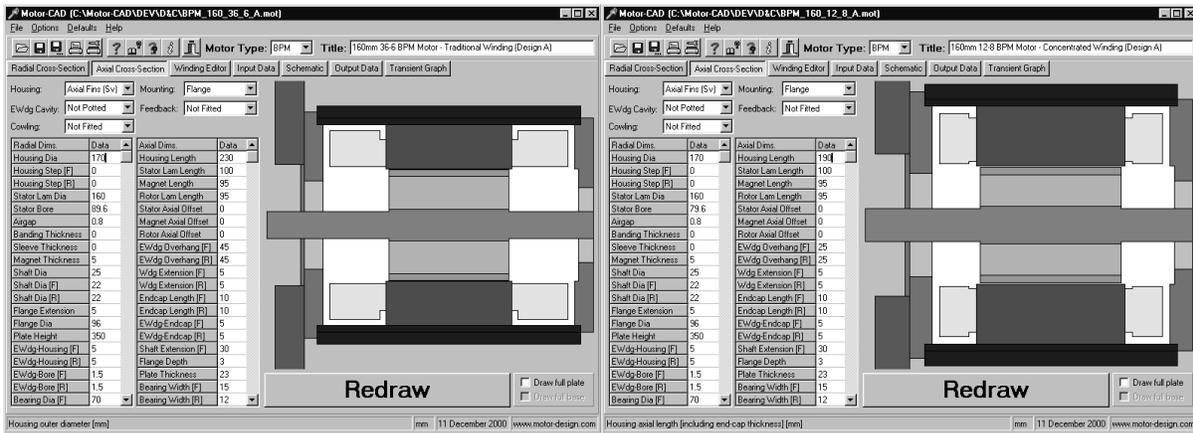
3

Fig. 5: Axial cross-section of 160mm diameter traditional & concentrated winding motor designs

Winding Design:

It is not practical to model each conductor so the slot-liner/copper/insulation layered winding model illustrated in Figs 6 & 7 has been developed. This enables the prediction of winding hotspots in the centre of the coil and the estimation of the short time constant associated with the winding rather than that of the whole motor (Fig 13). The number of layers and copper to insulation thickness ratio is set by wire diameter, number of turns and subsequent slot-fill. The winding diagrams are useful for gaining a visual indication of the slot-fill which can be achieved using various winding techniques.

Concentrated Winding Techniques:

Fig 6 shows the windings used in 80mm diameter motor designs shown in Figs 2 & 3. The winding on the left hand side is that of a traditional winding in which the coils are inserted into the slots through the slot openings. The winding on the right hand side shows the increased slot fill that can be achieved using a modern concentrated winding. Non-overlapping coils (bobbin winding) are precision wound directly onto a segmented tooth, the teeth are then joined together to form a wound stator [4]. Fig 7 shows the windings associated with the 160mm diameter designs shown in Figs 4 & 5.

The traditional winding process of inserting coils into the slots through the slot openings results in a random placement of conductors. A slot-fill limit of around 55% is achievable using this technique (based on round covered conductors and slot area available for winding after liner insertion). The concentrated winding technique presented here allows precision placement of conductors and slot-fills of around 80% can be achieved using this technique.

The motor axial cross-sections shown in Figs 3 & 5 also indicate that the non-overlapping winding benefits from having a shorter end-winding length. Not only does this result in a shorter motor, but also a reduction in resistance and copper loss. For example, in the case of the 80mm diameter motor designs, the concentrated winding design has a 100mm overall length compared to 130mm for traditionally wound motor. It also produces 34% more torque for the same temperature rise. In the case of the 160mm diameter motor designs, the concentrated winding design has a overall length of 190mm compared to 230mm for the traditional wound design. However, the torque increase for a given temperature rise is only 8%. The reduced improvement is largely due to the fact that the 36-slot traditional motor has 80% more total slot periphery than the 12-slot concentrated winding motor to dissipate its copper. In the case of the 80mm motors, the 18-slot motor has only a 16% benefit in terms of total slot periphery compared to the 12-slot motor. For this reason a larger slot number may be beneficial in the larger diameter motor, probably a 16-slot 18-pole or a 24-slot 16-pole design. The 16-slot 18-pole benefits from not requiring skew, the 24-slot 16-pole and 12-slot 8-pole designs needing to be skewed by half a slot pitch. The increased pole number would however lead to increased iron loss, although these are closer to the outside of the motor and would be easier to dissipate. These design possibilities will be investigated in the future.

Additional methods used to increase the winding dissipation include improved winding impregnation techniques and potting of the end-windings. Vacuum impregnation can eliminate air pockets within the winding. For instance the windings shown in Fig 5 benefit from a decrease in temperature rise of around 9% when the motors are perfectly impregnated compared to a 50% impregnated motor. The previous examples

4

use a traditional impregnation material having a thermal conductivity of 0.2W/m/C. However, new high temperature impregnation and potting materials are now available which have thermal conductivites of around 1W/m/C. If one of the new materials were to be used in the two designs shown in Fig 5, a reduction in temperature rise of between 6% and 8% could be expected. If the end-windings were potted, a reduction in temperature rise of between 14% and 16% would be expected.
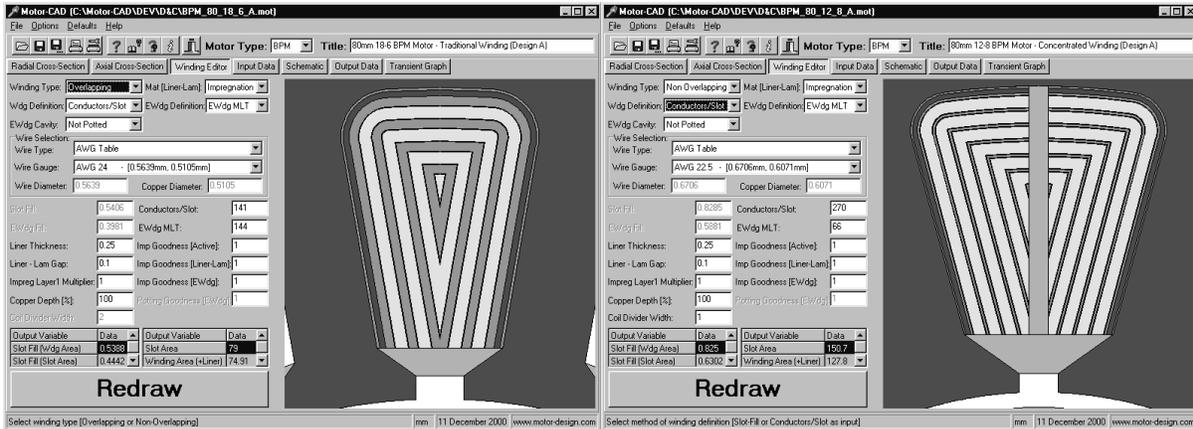

Fig. 6: Winding thermal model showing copper/insulation layers used in 80mm diameter traditional & concentrated winding motor designs
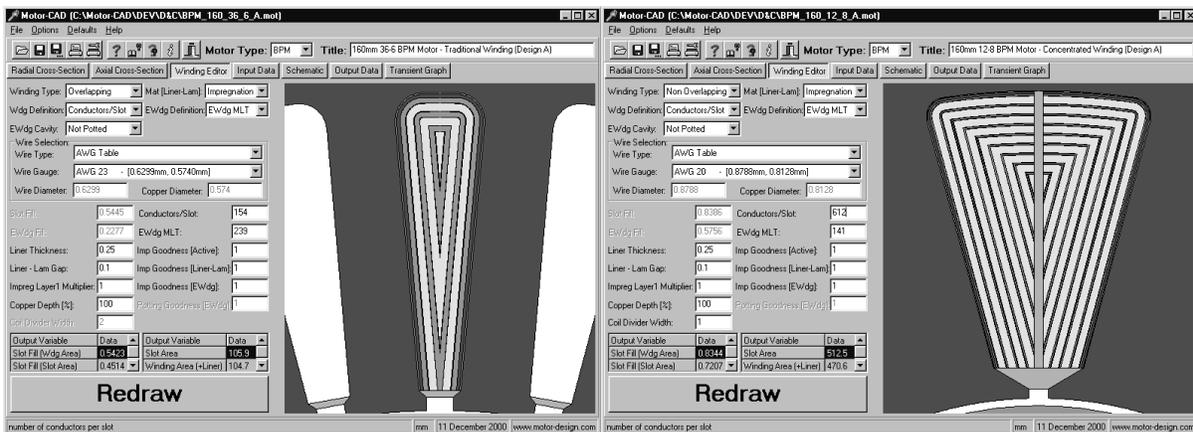

Fig. 7: Winding thermal model showing copper/insulation layers used in 160mm diameter traditional & concentrated winding motor designs

Thermal Mathematical Models:

Motor-CAD features efficient, accurate and robust mathematical algorithms for forced & natural convection, radiation and conduction. The particular convection model used for the various surfaces throughout the motor are automatically selected from a library of proven laminar and turbulent convection correlations [12-20]. Correlation formulations for open and closed channels and external surfaces of various shapes and orientations are included. Totally enclosed non-ventilated (TENV) and totally enclosed fan cooled (TEFC) forms of cooling are included. However, as the correlation formulations used are based upon dimensionless analysis of heat transfer [15], they are also applicable to liquid cooling methods such as housing water jackets, shaft spiral grooves, wet rotor and wet stator cooling techniques. These are included in Motor-CAD. Rotation effects on convection cooling in the airgap are included within the model [19-20].

Fin Design:

The fin design is often given little attention in servo motors as they traditionally do not have a shaft mounted fan because they are intended to operate down to zero speed. However, the radial fin design shown in Fig 8 can be used to increase the amount of natural convection from the housing [10,11,23]. In the case of the 80mm diameter motors presented earlier, a reduction in temperature rise of around 10% can be achieved by

adopting a radial fin design. There are special radial fin designs which allow similar dissipation when the motor is mounted vertically as when mounted horizontally [10,23].
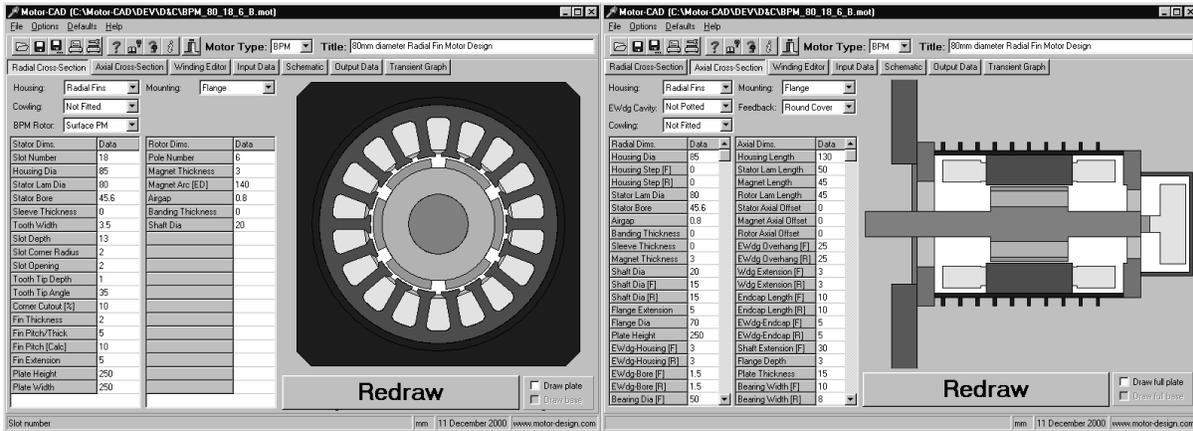

Fig 8: Motor with a radial fin design

External blower units are sometimes used to increase the output from servo motors [24]. If these are to be used, then one of the axial fin designs shown in Fig 9 would be beneficial.
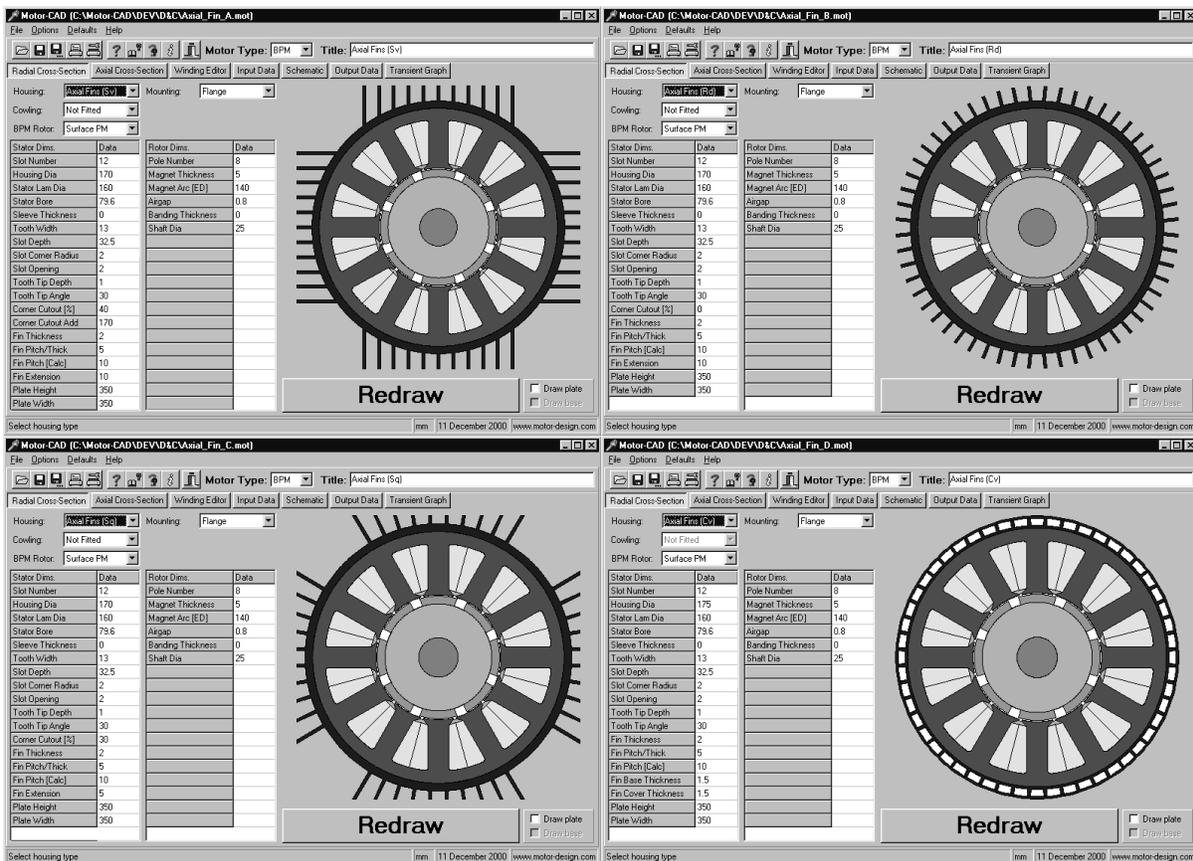

Fig 9: Examples of axial fin types available in Motor-CAD

Shaft mounted fans are often fitted to motors that are not intended for zero/low speed operation. In this case a cowling similar to that shown in Fig 10 is usually fitted to direct the air flow axially down the housing between the fin gaps.
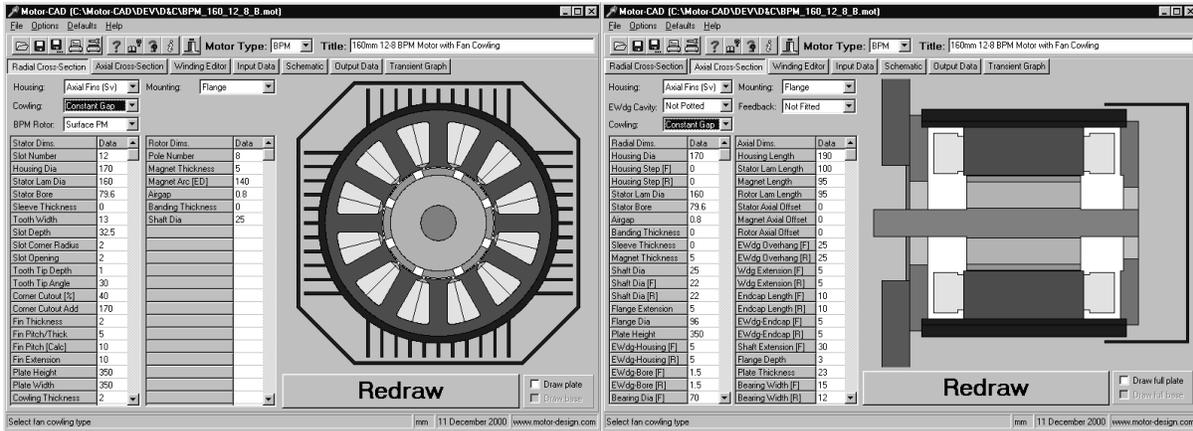
Fig 10: Example of cowling used in thermal model

Liquid Cooling:

For applications requiring the ultimate in terms of torque/volume a liquid cooling arrangement similar to those shown in Fig 11 can be adopted. Natural convection typically has a heat transfer coefficient (W/m/°C) of between 5 & 25, forced convection of between 10 & 300 and liquid cooling of between 50 & 20000 [14].
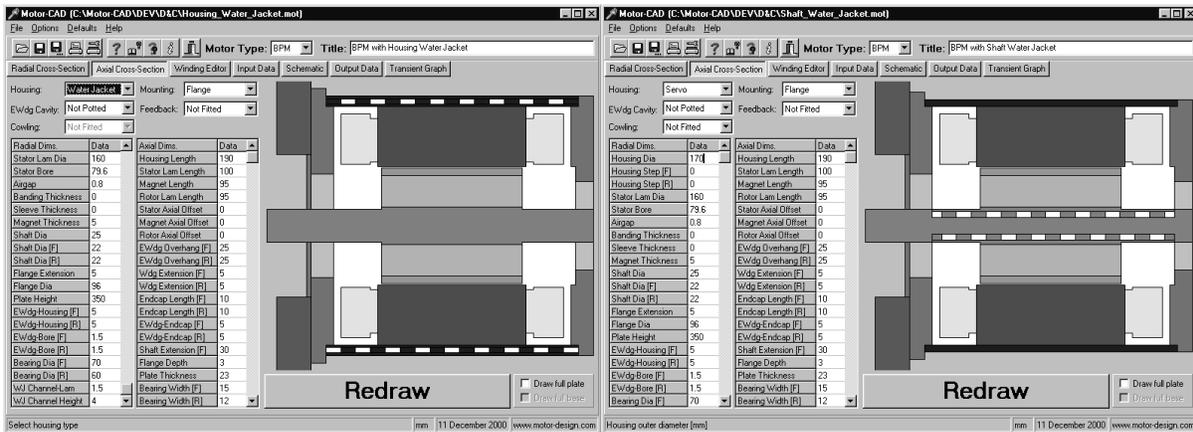

Fig 11: Example of liquid cooling arrangements available in Motor-CAD (housing & shaft water jackets)

Mounting Arrangement:

The mounting arrangement can have a significant impact on the thermal behaviour of the motor. In the servo motors shown in this paper, between 35 - 50% of the total loss is dissipated through the flange, the larger value being in the smaller motors. Such high figures are not uncommon as manufactures tend to use larger cooling plates than the standard plate sizes recommended by NEMA [22]. A motor must de-rate if it is unable to dissipate such powers into the device it is connected to.

Feedback Devices & Integrated Motors:

When an encoder is used as a feedback device then this should be included in the model as they typically have temperature limits of between 80°C and 100°C. The encoder model used in Motor-CAD is shown in Figs 1 & 3. The encoder model can also be adapted to predict the temperature rise of control and power electronics attached to the rear of motors in integrated motor drives [21].

Magnet Temperature Limit:

The magnet temperature is a key item to be calculated in permanent magnet motors, especially when Nd-Fe-B magnets are being used. This is because they are more sensitive to demagnetisation at elevated temperatures than Sm-Co. They also have a larger negative temperature coefficient of remanence which can

7

lead to a significant reduction in torque/amp (Kt) at high temperatures. The trend is that the higher remanence Nd-Fe-B materials which are suited to high power densities also have a lower BH knee value so are more prone to demagnetisation. However new grades of Nd-Fe-B are emerging which have relatively high remanence (1.19T) and linear 3rd quadrant BH characteristics up to 180°C [25]. It is reassuring that the magnets are somewhat isolated from the main sources of loss (i.e. the stator copper and iron loss), so that under a severe overload condition, the magnet temperature rise is much slower than that of the stator components (Fig 13).

Transient Analysis:

When carrying out transient analysis, thermal capacitances are connected to each of the nodes within the schematic shown in Fig 1. Each capacitance is calculated from the specific heat capacity and weight of the relevant motor components. The resulting set of partial differential equations are integrated to obtain the thermal transient characteristics.

Typical transient graphs are shown in Figs 12 & 13. Fig 12 shows the thermal transient produced when a motor is run at constant torque until the motor reaches its steady state temperature. It also shows the typical level of correspondence expected between measured and calculated transient characteristics when using Motor-CAD. It is also interesting to note that as with most motor rating tests, the motor current must be varied throughout the test to accommodate the torque constant (Kt) and iron losses which both reduce as the magnets heat up. These effects, in addition to the increase in winding resistance with temperature and the variation in losses with speed, are all taken account of within the program.

The transient graph shown in Fig 13 shows changes in temperature of the different motor components when driving a complex duty-cycle load. The duty-cycle editor used to describe the load is shown in Fig. 14. Duty-cycle analysis is essential in the majority of servo applications if the motor is to be driven to full potential without over-heating. This is illustrated in Figs 12 and 13 as the same motor is used for both calculations. When run continuously at rated torque the winding takes nearly 2 hours to reach its steady-state temperature. However when a severe duty cycle is used to load the machine, the same temperature is reached in around 100 seconds.
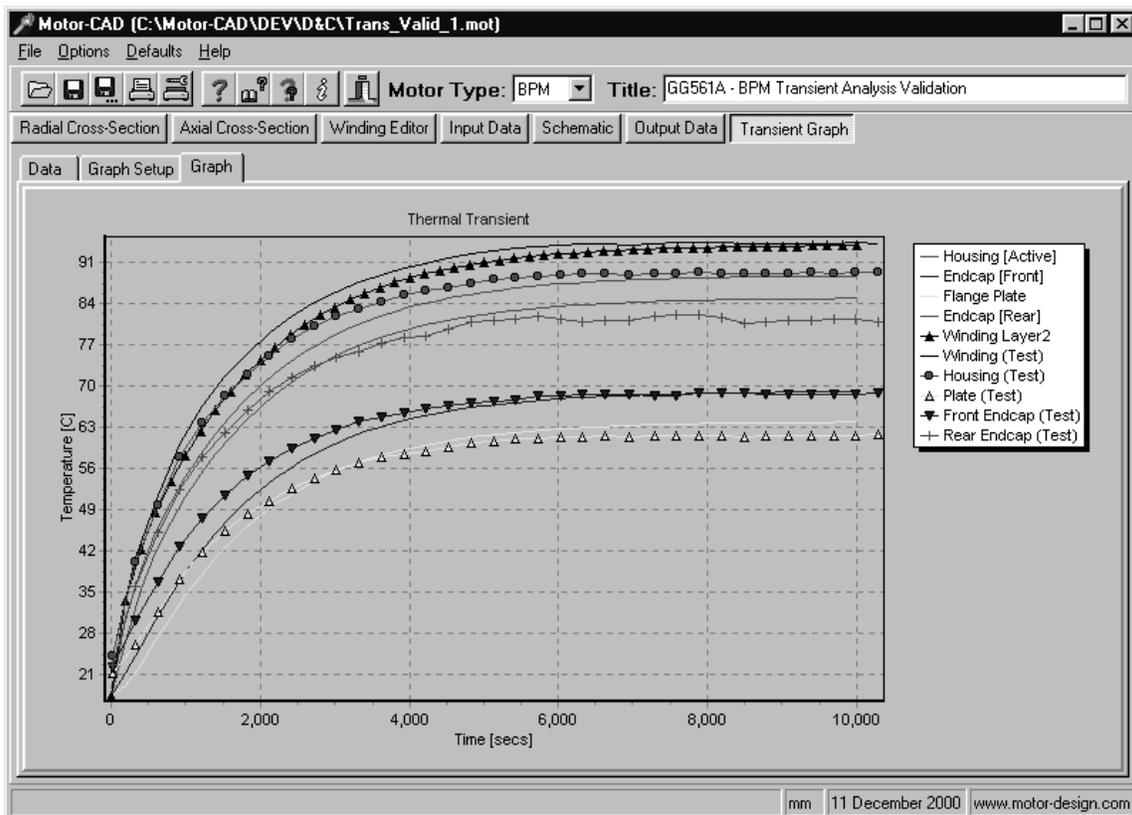

Fig. 12: Comparison of measured and calculated thermal transient for a small servo motor

8

CONCLUSIONS

This paper clearly demonstrates the advantages that can be gained from properly analysing the thermal characteristics of electric motors at the design stage. Motor-CAD has been developed as a tool to assist the designer in this complex and important area of design. Some examples of how thermal analysis can aid the miniaturisation of permanent magnet motors have been shown, supported by data where appropriate.

Motors-CAD transient calculation capabilities have been demonstrated with test data. If a motor is to be driven to full potential without over-heating, the importance of carrying out transient duty-cycle analysis has also been shown.
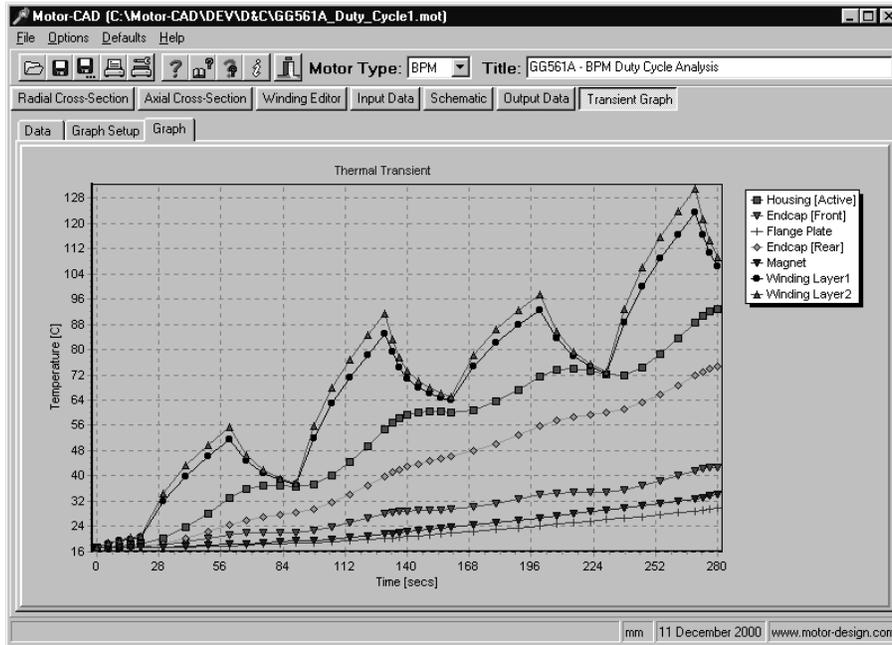

Fig. 13: Thermal transient for a small servo motor operating a duty cycle type load (load shown in Fig 14).
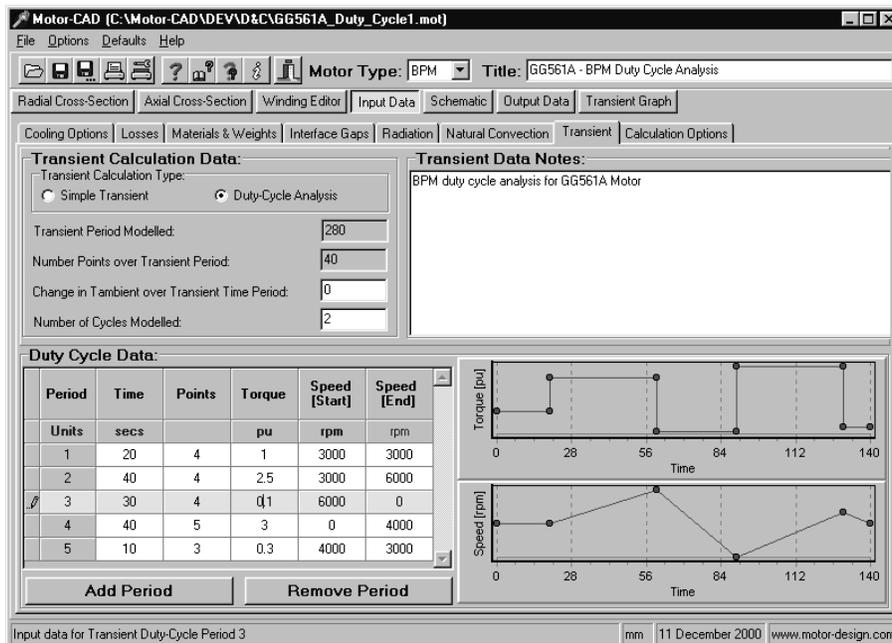

Fig. 14 Duty-cycle load editor

REFERENCES

[1]   AC Servo Drive ΣSeries, Yaskawa Product Brochure No. CHE-5800-18B

[2]   Technology Update - Servo Motors Double the Power Density, Drives & Controls, Jan. 2000

[3]   Compact Servos Boost Throughput, Drives & Controls, Sept. 2000

[4]   Compact Servo Motors, OEM Design, June 1995

[5]   AC motors are a third of the size, Drives & Controls Oct. 2000

[6]   Swedes Shrink Servomotors, Drives & Controls, April. 2000

[7]   Hendershot, J.R., Miller, T.J.E.: Design of Brushless Permanent-Magnet Motors, Magna Physics & Oxford Science Publications, 1994

[8]   Hanselman, D.C.: Brushless Permanent-Magnet Motor Design, McGraw-Hill, 1994

[9]   Hamdi, E.S.: Design of Small Elecrtical Machines, Wiley, 1994.

[10]   Staton, D.A., So E.: Determination of Optimal Thermal Parameters for Brushless Permanent Magnet Motor Design, IEEE-IAS Conference, St.Louis, Oct. 1998

[11]   Staton, D.A.: Thermal Analysis of Naturally Ventilated Servo Motor Housings, 5th International Flotherm User Conference, Paris, 16-19 Sept. 1996.

[12]   Ozisik, M.N.: Heat Transfer - A Basic Approach, McGraw Hill, 1995.

[13]   Simonson, J.R.: Engineering Heat Transfer, Macmillan, 1988.

[14]   White, F.M., Heat and Mass Transfer, Addison-Wesley.

[15]   Janna, W.S., Engineering Heat Transfer (S.I. Edition), Van Nostrand Reinhold (International), 1988

[16]   Bejan, A., Heat Transfer, John Wiley & Sons, Inc., 1993

[17]   Incropera, F.P., DeWitt, D.P., Introduction to Heat Transfer, John Wiley & Sons, 1990

[18]   Mellor, P.H., Roberts, D., Turner, D.R.: Lumped Parameter Thermal Model for Electrical Machines of TEFC Design. IEE Proc-B, Vol. 138, No. 5, Sept 1991.

[19]   Taylor, G.I.: 'Distribution of Velocity and Temperature between Concentric Cylinders', Proc Roy Soc, 1935, 159, PtA, pp 546-578

[20]   Gazley, C.: 'Heat Transfer Characteristics of rotating and axial flow between concentric cylinders', Trans ASME, Jan 1958, pp.79-89.

[21]   Technology Update, Drives & Controls, May 2000

[22]   Nema Standards:, Publication No. MG7, Revision Jan. 26, 1993.

[23]   Unimotor knocks the competition out cold, Torqueback magazine, Control Techniques Dynamics Ltd, Vol 1, Issue 3.

[24]   Fan cowlings boost torque by up to 87%, Drives & Controls, Oct. 1999.

[25]   Sumitomo Numax Catalogue, 1999